



*Citation for published version:*

Chuck, CJ, Jenkins, RW, Bannister, CD, Han, L & Lowe, JP 2012, 'Design and preliminary results of an NMR tube reactor to study the oxidative degradation of fatty acid methyl ester', *Biomass and Bioenergy*, vol. 47, pp. 188-194. <https://doi.org/10.1016/j.biombioe.2012.09.043>

*DOI:*

[10.1016/j.biombioe.2012.09.043](https://doi.org/10.1016/j.biombioe.2012.09.043)

*Publication date:*

2012

*Document Version*

Peer reviewed version

[Link to publication](#)

NOTICE: this is the author's version of a work that was accepted for publication in *Biomass and Bioenergy*. Changes resulting from the publishing process, such as peer review, editing, corrections, structural formatting, and other quality control mechanisms may not be reflected in this document. Changes may have been made to this work since it was submitted for publication. A definitive version was subsequently published in *Biomass and Bioenergy*, 2012, vol 47, DOI 10.1016/j.biombioe.2012.09.043

## University of Bath

### General rights

Copyright and moral rights for the publications made accessible in the public portal are retained by the authors and/or other copyright owners and it is a condition of accessing publications that users recognise and abide by the legal requirements associated with these rights.

### Take down policy

If you believe that this document breaches copyright please contact us providing details, and we will remove access to the work immediately and investigate your claim.

1 **Design and preliminary results of an NMR tube reactor to study the oxidative**  
2 **degradation of Fatty Acid Methyl Ester**

3 Christopher J. Chuck,<sup>a\*</sup> Rhodri W. Jenkins,<sup>a</sup> Chris D. Bannister,<sup>b</sup> Lu Han<sup>c</sup> and John P. Lowe<sup>c</sup>

4  
5 <sup>a</sup> Centre for Sustainable Chemical Technologies, Department of Chemical Engineering,  
6 University of Bath, Bath, UK, BA2 7AY.

7 <sup>b</sup> Department of Mechanical Engineering, University of Bath, Bath, UK, BA2 7AY.

8 <sup>c</sup> Department of Chemistry, University of Bath, Bath, UK, BA2 7AY.

9

10 \*email C.Chuck@bath.ac.uk, tel: +44 (0)1225 383537, fax: +44 (0)1225 386231

11 **Abstract**

12 Biodiesel is the fatty acid alkyl esters produced by the transesterification of vegetable,  
13 animal or microbial lipids. After ethanol, it accounts for the largest proportion of global  
14 biofuel production. Yet, due to the level of polyunsaturation, biodiesel is also oxidatively  
15 unstable. When biodiesel oxidizes the viscosity increases, which leads to reduced fuel  
16 performance and in extreme cases can lead to engine failure. To aid in understanding the  
17 process of this degradation a specialist NMR tube rig was designed to assess the oxidation of  
18 biodiesel. The NMR tube rig allowed the *in situ* <sup>1</sup>H NMR measurement of the sample while  
19 air was bubbled through at fixed intervals. The methyl esters of linolenic acid (18:3), linoleic  
20 acid (18:2) and oleic acid (18:1) were oxidised at 110 °C over a 24 hour period. The  
21 decomposition of biodiesel is complex, and there is more than one mechanism involved in  
22 the degradation. Using this rig the onset of oxidation for 18:3 and 18:2 was found to be  
23 almost instantaneous. The rate of oxidation was found to be slightly less for 18:2 than 18:3

1 while the maximum rate was observed for 18:3 from the beginning of the oxidation, this  
2 was only observed after 280 mins for 18:2. The oxidation of 18:1 started at approximately  
3 500 minutes and, slowly degraded during the remaining reaction time. The formation of a  
4 number of secondary oxidation products such as aldehydes, ketones, alcohols and formates  
5 were also quantified.

6

## 7 **1 Introduction**

8 Due to the increasing pressure to reduce greenhouse gases and the growing scarcity of fossil  
9 fuels, alternatives to liquid transport fuels are being increasingly sort. One such fuel is  
10 biodiesel, the fatty acid alkyl esters (FAAE) derived from the transesterification of vegetable,  
11 waste, animal or microbial lipids. Biodiesel has comparable properties to diesel fuel and, as  
12 such, can be used as a substitute for petroleum diesel in compression ignition engines.  
13 However, biodiesel is generally high in polyunsaturated esters which are prone to oxidation.  
14 As the fuel degrades volatile acids are given off, the viscosity increases substantially and  
15 eventually solid particles and gums are formed [1]. This is problematic as the oxidised fuel  
16 can block filters and injectors as well as leading to poor combustion and an increase in toxic  
17 emissions such as particulate matter (PM), polyaromatic hydrocarbons (PAH),  
18 formaldehyde, acetaldehyde and acrolein [2]. This problem is further exacerbated on  
19 modern vehicles equipped with a diesel particulate filter (DPF) where the fuel will slowly  
20 accumulate in the engine sump oil during filter regeneration events. While petroleum diesel  
21 will generally evaporate at the normal working temperature of the lubricating oil, and be  
22 recirculated back into the engine intake air for combustion, the biodiesel will persist and  
23 degrade, necessitating a premature oil change [3].

1           The rate of oxidation of biodiesel is dependent on many factors including the air  
2 available, metal content, temperature, light and most importantly the fatty acid profile [4,  
3 5]. The most common fatty acids found in biodiesel are palmitic acid (16:0), stearic acid  
4 (18:0), oleic acid (18:1), linoleic acid (18:2) and linolenic acid (18:3). The oxidative stability  
5 increases with increasing saturation and, as such, biodiesel rich in saturated esters such as  
6 palm or coconut oil methyl ester containing palmitic acid, tend to be more stable than those  
7 rich in polyunsaturates such as soybean oil methyl ester which is predominantly made up of  
8 linoleic and linolenic acids [6].

9           The oxidation of unsaturated lipids has been extensively researched previously with  
10 studies detailing the reaction of triglycerides and related compounds, the effect of the  
11 oxidation of lipids on appearance, flavor and toxicity as well as the role of natural anti-  
12 oxidants in these processes [7, 8]. More recently research has primarily been focused on  
13 detailing the oxidation of biodiesel [9]. From these studies FT-IR spectroscopy [10, 11], UV-  
14 VIS spectroscopy [12], GC-MS [13], peroxide or acid value and NMR spectroscopy have all  
15 been used to assess the decomposition [14, 15]. Though a number of mechanisms have  
16 been proposed detailing how biodiesel can degrade, it seems clear that the primary  
17 mechanism, the auto-oxidation, proceeds with the formation of a radical hydrocarbon  
18 species on the bisallylic carbon. This is followed by isomerization into a more stable  
19 structure. This radical will then react with oxygen in the air to form a peroxide species which  
20 further propagates the reaction. The peroxides can then break down into oxygenated  
21 intermediates which further degrade into small chain acids, ketones, alkenes and aldehydes  
22 [16]. The peroxide species' can also form dimers and oligomers [17]. However, further work  
23 has shown that an oligomeric peroxide species, with more than one peroxide linker, can also  
24 be formed which propagates the reaction by rapidly breaking down into aldehydes, acids

1 and an alkoxy radical species [18]. These aldehydes are unsaturated if the oxidised chains  
2 are joined by multiple peroxide linkers [19]. NMR spectroscopy has the potential to provide  
3 significant new information on biodiesel oxidation, but the few studies utilizing this  
4 technique that have been reported so far have used bench-top sampling techniques rather  
5 than *in situ* NMR experiments. Therefore, to further investigate the products and kinetics in  
6 the oxidation of biodiesel, a rig was designed to allow the *in situ* analysis of the oxidation of  
7 pure FAME samples via  $^1\text{H}$  NMR spectroscopy.

8

## 9 **2 Experimental**

### 10 **2.1 Materials**

11 Deuterated xylene and dodecane were purchased from Fluorochem, oleic acid methyl ester,  
12 18:1, (99.0%), linoleic acid methyl ester, 18:2, (99.0%) and linolenic acid methyl ester, 18:3,  
13 (99.0%) were purchased from Sigma-Aldrich and used without further purification. All  
14 chemicals were stored at  $-85\text{ }^\circ\text{C}$  prior to use.

15

### 16 **2.2 $^1\text{H}$ NMR spectroscopy method**

17 The NMR rig was created using standard silicone tubing, glass and polycarbonate casing with  
18 Teflon seals. NMR spectroscopic measurements were carried out at 383 K using a Bruker  
19 AV500 spectrometer, operating at 500.13 MHz for  $^1\text{H}$ . Standard Bruker pulse sequences  
20 were used throughout.  $^1\text{H}$  spectra were typically acquired using a 30 degree excitation pulse  
21 and a repetition time of 4.2 sec. 1.0 Hz line broadening was applied before Fourier  
22 transform, and spectra were referenced to the residual xylene solvent peak ( $\delta$  6.90 ppm).

23 In a typical run, FAME (0.05 ml) was added to deuterated xylene (0.9 ml) and  
24 deuterated dodecane (0.05 ml) in the NMR tube rig, which was held statically in the NMR

1 machine. The temperature of the NMR machine was set to 110 °C and allowed to stabilize.  
2 The NMR rig was then inserted into the NMR machine, the sample was shimmed and an  
3 NMR spectrum was recorded. This was taken as time = 0. Air was bubbled through the tube  
4 at a rate of 1 ml min<sup>-1</sup> over a period of 8 minutes using a peristaltic pump with automated  
5 control settings, after which the mixture was allowed to settle for 2 mins. During this time,  
6 a <sup>1</sup>H NMR spectra was recorded. This process was repeated over a 24 hour period, with both  
7 the pump and the data acquisition under automated control. After processing, the spectra  
8 were integrated relative to the residual solvent peak of the xylene which was found to differ  
9 by less than 3.5% throughout the course of the reaction. Three replicates of the reaction  
10 were run to assure the consistency of the data.

11 To aid in the assignment of the oxygenated products, COSY, HSQC and HMBC  
12 experiments were undertaken on a sample of 18:2 after 500 min reaction time. The sample  
13 was oxidized under the conditions described above, the sample was then crash cooled to  
14 halt the oxidation and redissolved in CDCl<sub>3</sub> prior to analysis.

15

## 16 **3 Results and Discussion**

### 17 **3.1 Reactor Design**

18 In the oxidation of biodiesel, small chain organic acids are produced in significant quantities  
19 [20], therefore, the NMR tube rig was designed to be air-tight with a stable outlet to remove  
20 these volatiles from the reaction mixture. The tube reactor had not only to be acid resistant,  
21 but also stable at 110 °C. Glass, treated silicone tubing, teflon and polycarbonate were  
22 considered suitable materials. The reactor consisted of a standard glass NMR tube with  
23 screw top, a sealed polycarbonate casing was built around this allowing an air-tight inlet and  
24 outlet section fitted with silicone piping (Fig. 1).

1           As the silicone material has the potential to swell if infused with solvent, which  
2 would effectively seal the tube, a long glass rod was attached to the inlet. Solid materials  
3 such as the glass rod, as well as gas bubbles, degrade the homogeneity of the magnetic field  
4 and results in severe line broadening making quantification of the individual peaks difficult.  
5 One method to overcome this was to hold the inlet pipe above the region where the  
6 measurement was made, however, this technique resulted in poor mixing and a low  
7 interaction between the air and biodiesel. Instead the glass rod was held symmetrically in  
8 the centre of the tube by pushing it against the bottom. This had the added benefit of  
9 dispersing the gas bubbles and increasing the surface interaction between the two phases.  
10 This concentric tube arrangement gives reasonably good magnetic homogeneity and,  
11 without bubbling, the resulting spectra had acceptable NMR lineshapes. To reduce line  
12 broadening due to the gas bubbles, the air at  $1 \text{ ml min}^{-1}$ , was pumped through the system  
13 using a peristaltic pump running an automated program with 2 minutes of down time every  
14 10 minutes. This was shown to be sufficient to allow the mixture to settle and an NMR  
15 spectra to be recorded. The NMR spectra were recorded in a mixture of deuterated  
16 dodecane (5%) and xylene (95%), as it was thought this solvent mixture was a reasonable  
17 (cost permitting) model for diesel or engine oil fuel.

18

### 19 **3.2 Oxidation of pure FAME samples**

20 The main oxidative mechanism, the auto-oxidation, proceeds by the formation of a carbon  
21 radical on the bisallylic carbon, the double bonds then conjugate, to form a more stable  
22 system and the radical reacts with oxygen to form a peroxide species [7]. As there is no  
23 bisallylic site on 18:1, this mechanism is less favoured and other oxidative mechanisms can  
24 also be observed such as the formation of an epoxide [21]. The signal relating to

1 unconjugated double bonds ( $\delta$  5.3 – 5.5 ppm) can then be used to assess the degradation.  
2 Despite the absence of light in the NMR machine, the oxidation proceeds rapidly. 18:3  
3 begins to decompose immediately and by 600 minutes only 20% of the starting material  
4 remains (Fig. 2). 18:2 oxidises more slowly than the 18:3, though the onset of oxidation is  
5 almost immediate. There is no visible reduction in the double bonds of 18:1 until 500  
6 minutes into the reaction (Fig. 3a). After this point the double bonds slowly reduce. A similar  
7 trend is observed for the degradation of the bisallylic sites (Fig. 3b). After 24 hours of  
8 oxidation, less than 5% of the original sites remain in both 18:2 and 18:3.

9           In order to determine the instantaneous and maximum rate of degradation for each  
10 FAME type, it was necessary to remove noise from the raw data using filtering. Within the  
11 MatLab environment, a zero-phase digital filter was applied in both the forward and reverse  
12 directions (Fig. 4). The resultant filtered FAME concentration data was then differentiated to  
13 determine the rate of degradation and the maximum rate was identified along with the time  
14 at which it occurred. Table 1 summarises the rate data for each FAME type. As can be seen,  
15 the rate of decomposition is related to the structure, with 18:3 demonstrating the highest  
16 rate occurring almost instantaneously at the start of the test. 18:2 shows a very similar  
17 trend to 18:3, but its maximum rate of decomposition is not achieved until 280 minutes into  
18 the reaction. It would appear that 18:1 never achieves a maxima, as the rate of  
19 decomposition is continuing to increase even after 1430 minutes. Using the NMR reactor  
20 the maximum rate of the oxidation of 18:2 and 18:3 is highly similar while the degradation  
21 of 18:1 was found to be five times lower.

22

### 23 **3.3 Analysis of secondary products**

24



1 Some of the major secondary products in the oxidation of biodiesel are aldehydes. These  
2 components are observed during the decomposition in relatively large quantities for the  
3 oxidation of the polyunsaturated FAMES (Fig. 5). In the oxidation of 18:1, small amounts are  
4 observed on degradation of the double bonds and it seems likely that the aldehydes are also  
5 a decomposition product from the oxidation of the monounsaturated component. In the  
6 degradation of 18:2 and 18:3, aldehydes are produced from the onset, reach a maxima at  
7 roughly 500 minutes into the reaction time, and then both reduce slowly over the remaining  
8 time.

9         The reduction in the aldehyde peak corresponds with the decrease in the rate of  
10 double bonds being consumed. Aldehydes are a primary decomposition product from the  
11 oxidative breakdown of lipids, and previous studies have shown, that on the oxidation of  
12 polyunsaturated lipids, a range of unsaturated and saturated aldehydes are formed on the  
13 oxidation of the pure lipids [8]. To further assess the applicability of using NMR to aid in the  
14 assignment of these oxygenates, COSY, HSQC and HMBC NMR experiments were  
15 undertaken (given in the supporting information). COSY spectra show which protons are  
16 coupled to each other, and therefore typically on adjacent carbon atoms. Such coupling is  
17 indicated by the presence of cross-peaks (off-diagonal peaks) at the chemical shift of one  
18 proton on the vertical axis and its coupled proton on the horizontal axis. In the resulting  
19 COSY plot it can be seen that a minority of the aldehyde protons at 9.4 – 9.8 ppm are  
20 coupled to the protons of saturated carbon chains at 2.4 ppm, whereas the majority are  
21 coupled to alkenic protons at 6.1 – 6.4 ppm.

22         Likewise, HSQC spectra reveal the chemical shift of the carbon atoms directly  
23 bonded to each proton. Since  $^{13}\text{C}$  chemical shifts are spread out over a greater range than  $^1\text{H}$   
24 chemical shifts, the  $^{13}\text{C}$  shift associated with a particular  $^1\text{H}$  resonance is often useful as a

1 diagnostic tool. By running an HSQC NMR experiment the majority of the protons were  
2 found to couple to carbonyl carbon atoms at around  $\delta$  194 ppm further suggesting that the  
3 majority of the aldehydes are unsaturated, the rest of the aldehydes coupled to a peak at  $\delta$   
4 204 ppm, suggestive of a saturated aldehyde This is supportive that the breakdown of 18:2  
5 follows from the decomposition of carbon chains with multiple peroxide linkers [19]. The  
6 oxidation of 18:2 using the NMR reactor produces over twice as many aldehydes than the  
7 decomposition of 18:3, this major difference is presumably due to the formation of more  
8 volatile components such as crotonaldehyde during the oxidation of 18:3, as opposed to  
9 longer less volatile components in the oxidation of 18:2, a mechanism proposed by Frankel  
10 and co-workers [8].

11 On the decomposition of biodiesel, formic acid is also produced [20]. The formic acid  
12 is volatile and will evaporate from the reaction mixture. In a previous study conducted on  
13 the oxidation of RME, a range of formates, in addition to formic acid, have been observed in  
14 the reaction mixture [21]. It was assumed that formic acid was being formed and reacting  
15 with alcohols, a further decomposition product in the oxidation. In the NMR tube reactor,  
16 only a minor amount of formic acid or formates are observed in the oxidation of 18:1 and  
17 18:3 (Fig. 6). Formic acid is present, but is presumably being removed from the system more  
18 efficiently due to the air flow. In the oxidation of 18:2 however, a number of peaks are  
19 observed in this region, suggesting that other types of formates are being produced in large  
20 quantities solely from the oxidative breakdown of this particular FAME, this assignment is  
21 supported up by the lack of coupling to any other protons in the COSY plot.

22 If a number of formate esters are being formed then the protons on the  $\alpha$ -carbon of  
23 the ester moiety will be observed between  $\delta$  3.7 and 4.5 ppm. Over the course of this study  
24 very little is observed in this region for 18:1 or 18:3, however, like the formate proton there

1 are a number of peaks found in this region for 18:2 (Fig. 7). Though protons attributable to  
2 ketones or aldehydes will not appear in this region other possibilities are peroxides, the  $\alpha$ -  
3 protons of an alcohol or the hydroxyl proton itself. It seems unlikely that the hydroxyl  
4 protons come in this area as the addition of D<sub>2</sub>O did not change the spectra (see supporting  
5 information). The HSQC plot demonstrates that the protons are bound to carbons with  
6 shifts between  $\delta$  68 - 86 ppm, this is consistent with them being attributable to the  $\alpha$ -  
7 protons of alcohols or formate esters. The COSY plot of this region shows that the majority  
8 of these protons are coupling to protons found in the region  $\delta$  1.5-1.7 ppm, with the rest  
9 coupled to alkenic protons. This suggests that though a majority of this signal corresponds  
10 to long chain saturated alcohols and formates, there are still a proportion of oxygenated  
11 products with a remaining double bond on the chain.

12 The oxygenates in this region reach a maxima at around 500 minutes into the  
13 reaction, after this point the concentration does not change to any significant degree (Fig.  
14 8). This is not the case in 18:3, suggesting that other products, unique to the breakdown of  
15 18:3, are themselves decomposing over the course of the reaction, but being produced in  
16 much lower quantities than for 18:2. For the oxidation of 18:1, the alcohol or formate  
17 components are observed as soon as the double bonds start to oxidise and this amount  
18 continues to increase throughout the reaction time, suggesting they represent a major  
19 decomposition product of the breakdown.

20 The other primary decomposition products in the oxidation of lipids are ketones [7,  
21 8]. Ketones can be identified by a characteristic shift between  $\delta$  2.45 – 2.75 ppm in the  
22 proton spectra. Aside from ketones however, ethers and epoxides will all have shifts in this  
23 region. However, the HSQC plot shows correlations to carbons at around  $\delta$  44 ppm, typical  
24 of ketones. Furthermore, the HMBC spectrum, which gives similar information to the HSQC

1 experiment except that it shows coupling from a particular proton to carbons two or three  
2 bonds away rather than one bond, shows coupling to carbonyl peaks found at  $\delta$  200 and 204  
3 ppm. This demonstrates that though ethers and epoxides can be formed in the oxidation of  
4 biodiesel [20, 21], they were not observed under these conditions. The ketones are  
5 observed in the decomposition of all the FAMEs analysed over the course of this study (Fig.  
6 9). The protons found in this region coupled entirely to protons observed at  $\delta$  1.5 - 1.6 ppm  
7 and not to any alkenic protons. This suggests that all the double bonds have reacted when  
8 these ketones are formed. The ketones were observed in the same molar percentage as the  
9 aldehydes although, unlike the aldehydes, the ketones appear to be a stable product of the  
10 oxidation. The oxidation of 18:3 produces the largest integral across this area, noticeably  
11 higher than that of 18:2.

12

#### 13 **4. Conclusions**

14 A specialist NMR rig was designed to further investigate the oxidation of pure FAME samples  
15 to further understand the pathways and decomposition products of biodiesel. 18:3 and 18:2  
16 were found to decompose almost instantaneously under the reaction conditions, though  
17 the rate of decomposition was at its highest at the beginning of the reaction for 18:3, this  
18 was not the case with 18:2. The decomposition of 18:1 was observed to only commence  
19 after 500 minutes of the reaction, at its highest the rate of decomposition was still  
20 approximately five times slower than for 18:2 or 18:3. In addition a larger quantity of  
21 aldehydes, esters, acids and alcohols were observed in the decomposition of 18:2 than in  
22 the other reactions, with the presence of these compounds suggesting that the breakdown  
23 of 18:3 produces more volatile components whereas 18:2 is breaking down through a  
24 number of mechanisms presumably forming oligomeric peroxide species with multiple

1 linkers. All the oxygenates were found to be a mix of saturated and unsaturated for 18:2 and  
2 18:3, with ketones seemingly being the most stable oxidation products.

3

#### 4 **5. Acknowledgements**

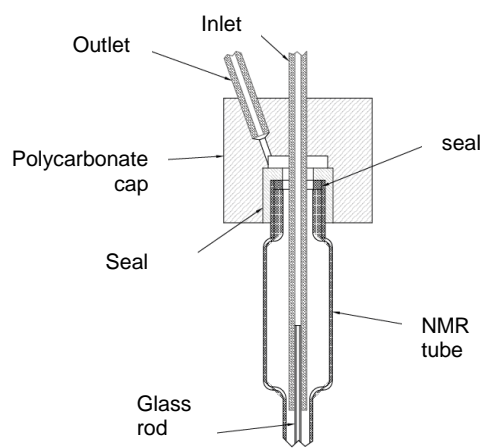
5 We would like to acknowledge the EPSRC for funding various aspects of this work, through  
6 the Doctoral Training Centre at the Centre for Sustainable Chemical Technologies, the Ford  
7 Motor Company for financial and material contributions, as well as Paul Firth and Phil Jones  
8 for their technical support throughout the project.

## 1 6. References

- 2 [1] Bannister CD, Chuck CJ, Bounds M, Hawley JG. Oxidative stability of biodiesel fuel. Proc Inst  
3 Mech Eng Part D-J Automob Eng 2011;225:99-114
- 4 [2] Karavalakis G, Bakeas E, Stournas S. Influence of Oxidized Biodiesel Blends on Regulated and  
5 Unregulated Emissions from a Diesel Passenger Car. Environ Sci Tech 2010;44:5306-12
- 6 [3] Fang HL, Whitacre SD, Yamaguchi ES, Boons M. Biodiesel impact on wear and protection of  
7 engine oils. SAE technical paper series 2007;2007-01-4141.
- 8 [4] Bannister CD, Chuck CJ, Hawley JG, Price P, Chrysafi SS. Factors affecting the decomposition  
9 of biodiesel under simulated engine sump oil conditions. Proc Inst Mech Eng Part D-J Automob Eng  
10 2010;224:927-40
- 11 [5] Knothe G, Dunn RO. Dependence of oil stability index of fatty compounds on their structure  
12 and concentration and presence of metals. J Am Oil Chem Soc 2003;80:1021-26
- 13 [6] Knothe G. Structure indices in FA chemistry. How relevant is the iodine value? J Am Oil Chem  
14 Soc 2002;79:847-54
- 15 [7] Frankel EN. Lipid Oxidation. 2nd ed. Dundee: Oily Press; 2005.
- 16 [8] Frankel EN. Lipid oxidation - mechanisms, products and biological significance. J Am Oil  
17 Chem Soc 1984;61:1908-14
- 18 [9] Dunn RO. Effect of oxidation under accelerated conditions on fuel properties of methyl  
19 soyate (biodiesel). Journal of the American Oil Chemists Society 2002;79:915-20
- 20 [10] Furlan PY, Wetzell P, Johnson S, Wedin J, Och A. Investigating the Oxidation of Biodiesel From  
21 Used Vegetable Oil by FTIR Spectroscopy: Used Vegetable Oil Biodiesel Oxidation Study by FTIR.  
22 Spectr Lett 2010;43:580-85
- 23 [11] De Lira LFB., de Albuquerque MS, Pacheco JGA, Fonseca TM, Cavalcanti EHS, Stragevitch L,  
24 Pimentel MF. Infrared spectroscopy and multivariate calibration to monitor stability quality  
25 parameters of biodiesel, Microchemical Journal, 2010;96:126-31.

- 1 [12] Dantas MB, Albuquerque AR, Barros AK, Filho MGR, Filho NRA, Sinfrônio FSM, et al.  
2 Evaluation of the oxidative stability of corn biodiesel. *Fuel* 2011;90:773-8
- 3 [13] Fang HL, McCormick RL. Spectroscopic study of biodiesel degradation pathways. SAE  
4 technical paper series 2006;2006-01-3300.
- 5 [14] Jain S, Sharma MP. Stability of biodiesel and its blends: A review. *Renew Sust Energ Rev*  
6 2010;14:667-78
- 7 [15] Knothe G. Analysis of oxidized biodiesel by H-1-NMR and effect of contact area with air. *Eur J*  
8 *Lipid Sci Technol* 2006;108:493-500
- 9 [16] Knothe G. Some aspects of biodiesel oxidative stability. *Fuel Process Technol* 2007;88:669-77
- 10 [17] Monyem A, Canakci M, Van Gerpen JH. Investigation of biodiesel thermal stability under  
11 simulated in-use conditions. *Appl Eng Agric* 2000;16:373-78
- 12 [18] Morita M, Tokita M. The real radical generator other than the main product hydroperoxide  
13 in lipid autoxidation. *Lipids* 2006;41:91-5
- 14 [19] Schneider C, Porter NA, Brash AR. Routes to 4-hydroxynonenal: Fundamental issues in the  
15 mechanisms of lipid peroxidation. *J Biol Chem* 2008;283:15539-43
- 16 [20] Ogawa T, Kajiya S, Kosaka S, Tajima I, Yamamoto M, Okada M. Analysis of Oxidative  
17 Deterioration of Biodiesel Fuel. SAE technical paper series 2008;2008-01-2502.
- 18 [21] Chuck CJ, Bannister CD, Jenkins RW, Lowe J, Davidson MG. A comparison of analytical  
19 techniques and the products formed during the decomposition of biodiesel under accelerated  
20 conditions. *Fuel* 2012;96:426-33

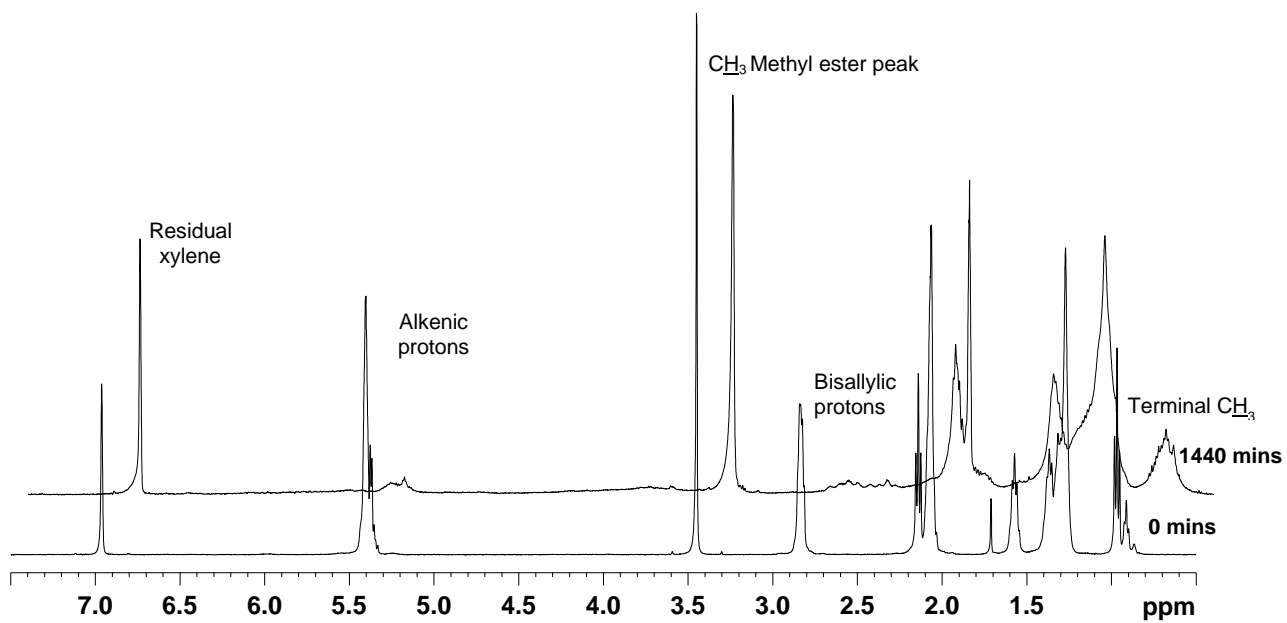
21



- 1
- 2
- 3
- 4
- 5

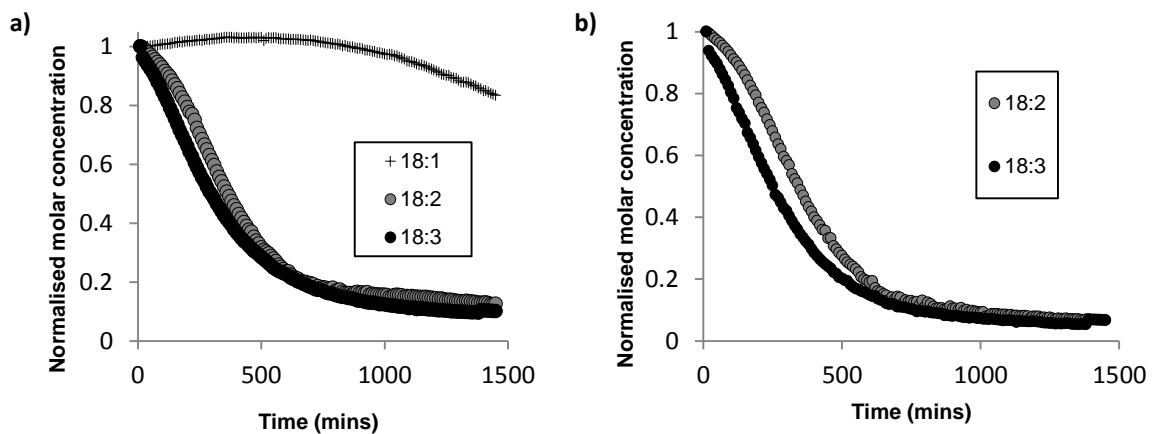
Figure 1. NMR tube reactor design





1  
2  
3  
4  
5

Figure 2. Representative  $^1\text{H}$  NMR spectra of 18:3, showing the spectra recorded at 0 and 1440 minutes, the upper spectra has been shifted to the right for clarity and is not to scale.



1

2

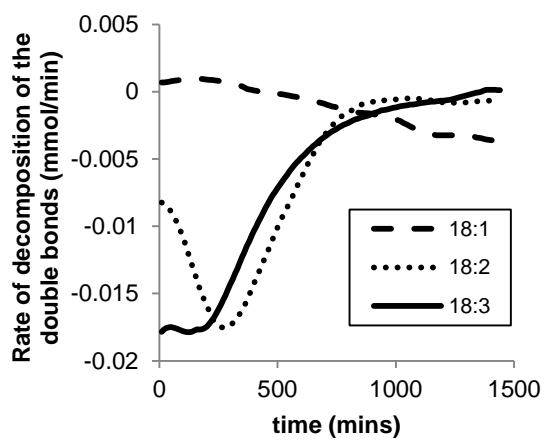
Figure 3. a) Reduction in the double bonds of 18:1, 18:2 and 18:3, b) reduction in the bisallylic

3

protons for 18:2 and 18:3

4

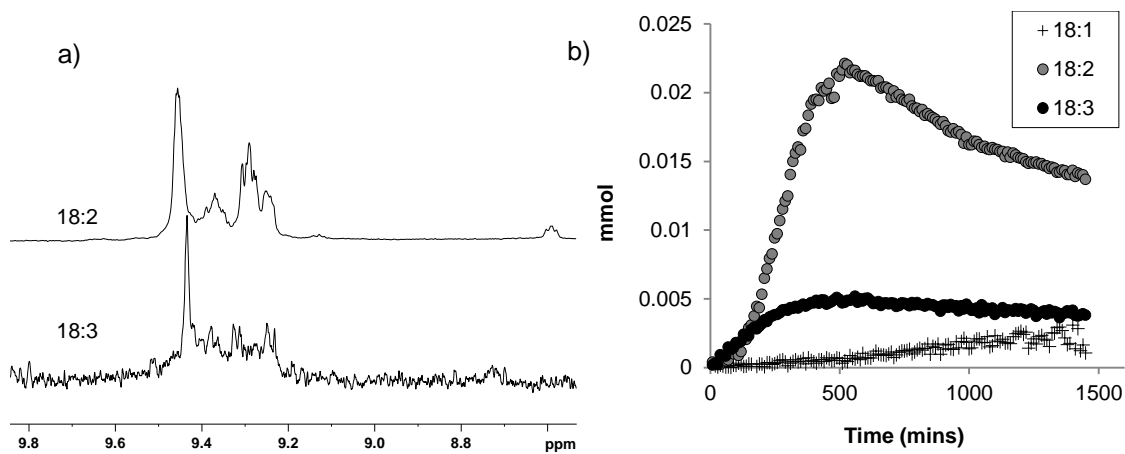
5



1

2 Figure 4 Rate of the consumption of double bonds throughout the reaction, by integration of the  
3 peak  $\delta$  5.3-5.5 ppm for the pure FAME samples 18:1, 18:2 and 18:3

4



1

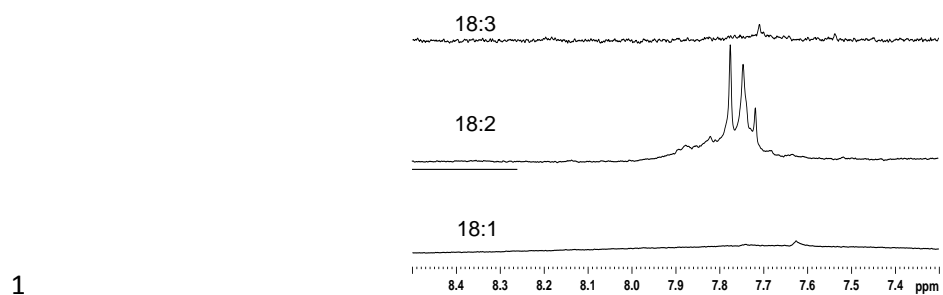
2 Figure 5 a) Aldehyde region ( $\delta$  9.0 – 9.5 ppm) of the <sup>1</sup>H NMR spectra after 8 hours oxidation, b)

3

aldehydes produced throughout the course of the reactions for 18:1, 18:2 and 18:3

4

5



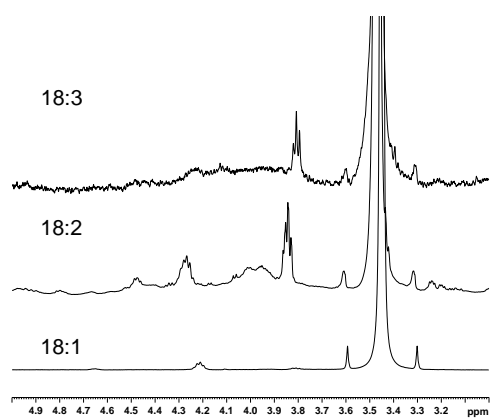
1

2

Figure 6. Formate region ( $\delta$  7.5 – 8.0 ppm) of the <sup>1</sup>H NMR spectra after 24 hours oxidation

3

4



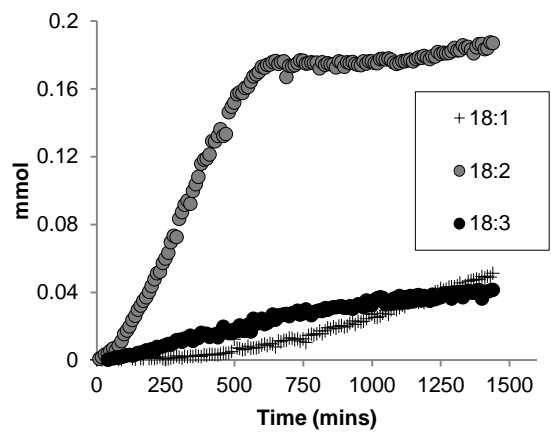
1

2 Figure 7 Region in the  $^1\text{H}$  NMR spectra ( $\delta$  3.7-4.5 ppm) attributable to the  $\alpha$ -protons on the esters

3 and alcohols formed after 500 minute reaction time

4

5

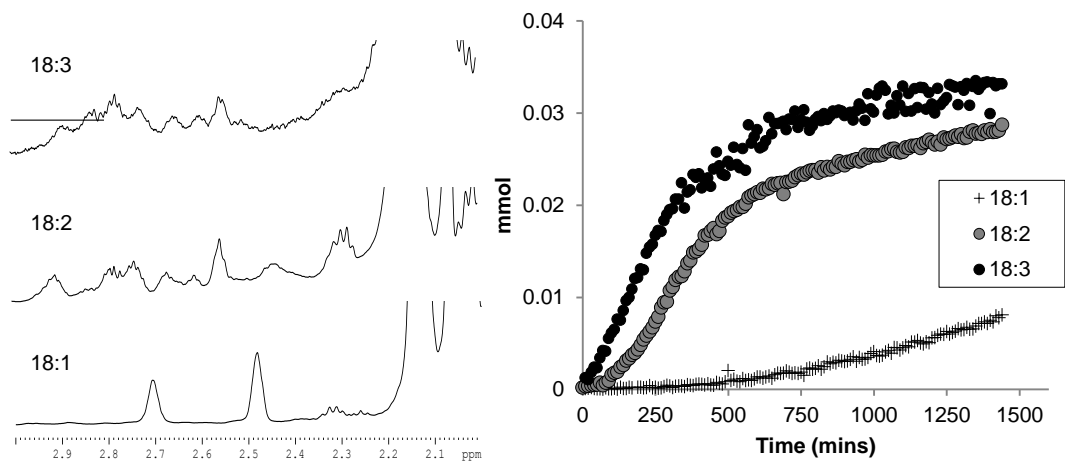


1

2 Figure 8. Integral plot of the region  $\delta$  3.7 - 4.6 ppm, predominated by the  $\alpha$ -protons of esters and  
3 alcohols produced throughout the course of the three reactions

4

5



1  
2  
3  
4  
5

Figure 9. The ketone region ( $\delta$  2.45-2.74 ppm) of the a) <sup>1</sup>H NMR spectra and b) the integral of the region plotted against time for the three FAME samples



<b>FAME Type</b>	<b>Time of Max. Rate (mins)</b>	<b>Max. Rate (mmol/min)</b>
<b>18:1</b>	<b>1430</b>	<b>-0.0037</b>
<b>18:2</b>	<b>280</b>	<b>-0.0175</b>
<b>18:3</b>	<b>130</b>	<b>-0.0179</b>

1

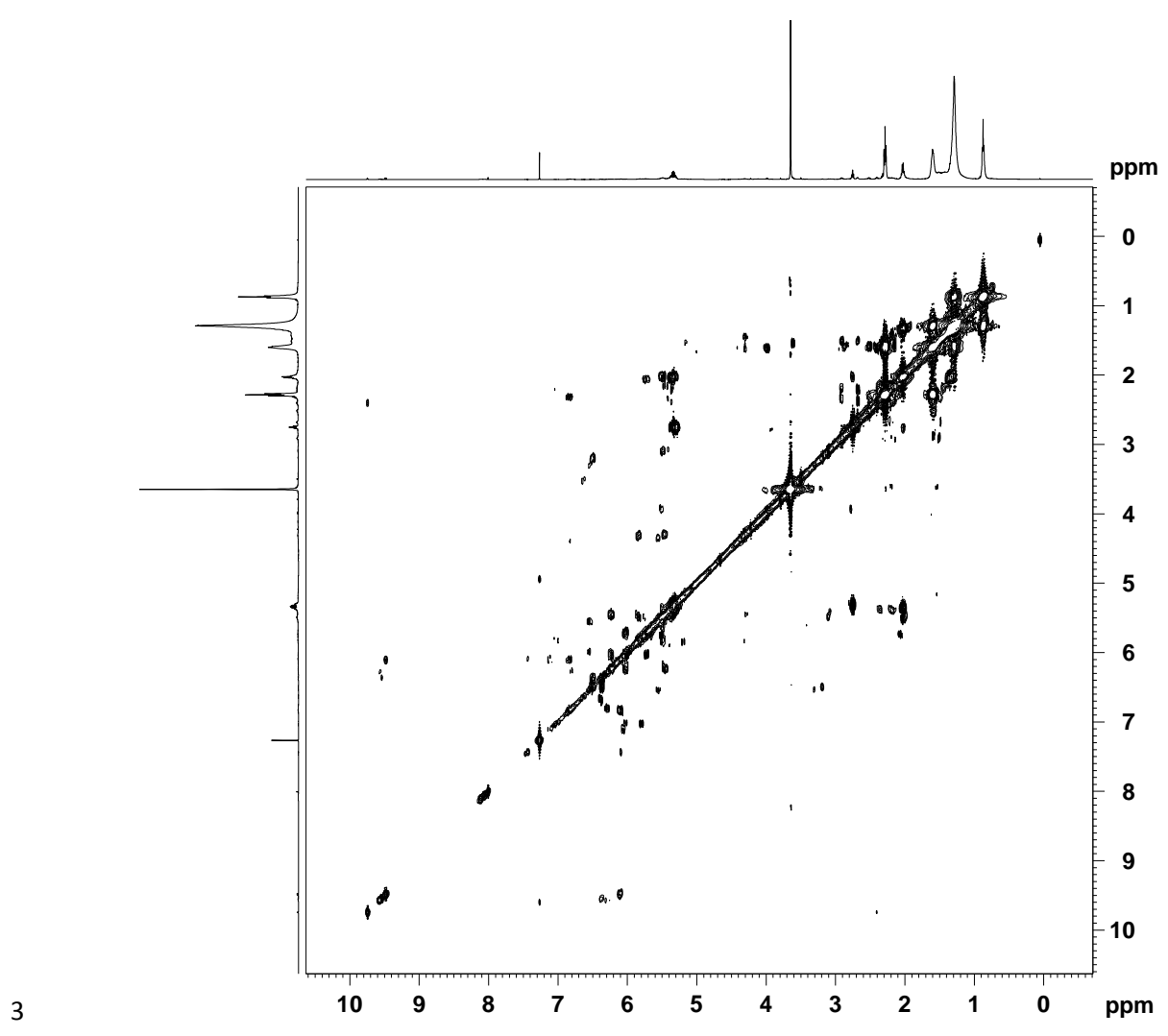
2 Table 1 – Rate of FAME degradation

3

4

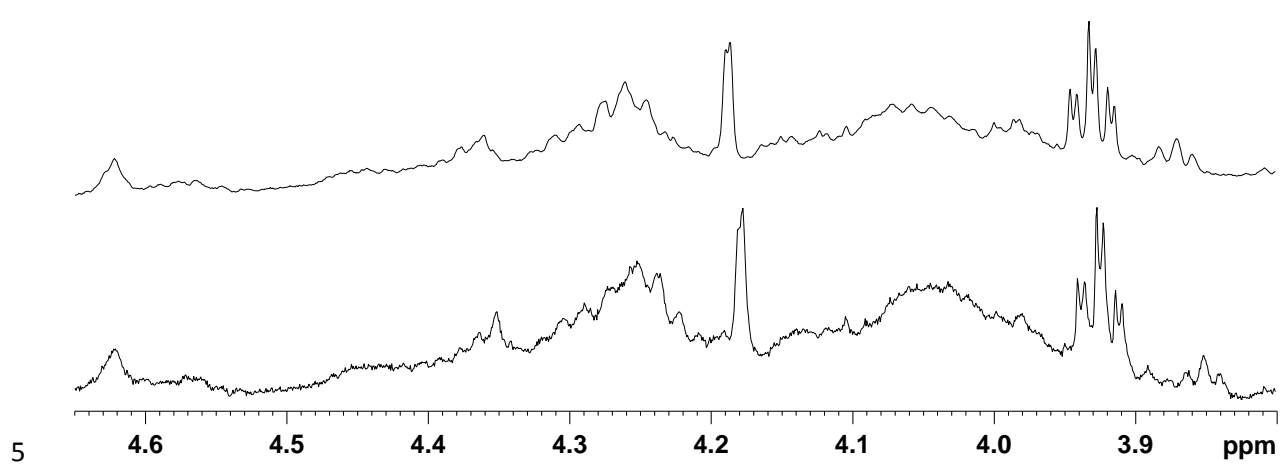
1

2 **Supplementary information**



3

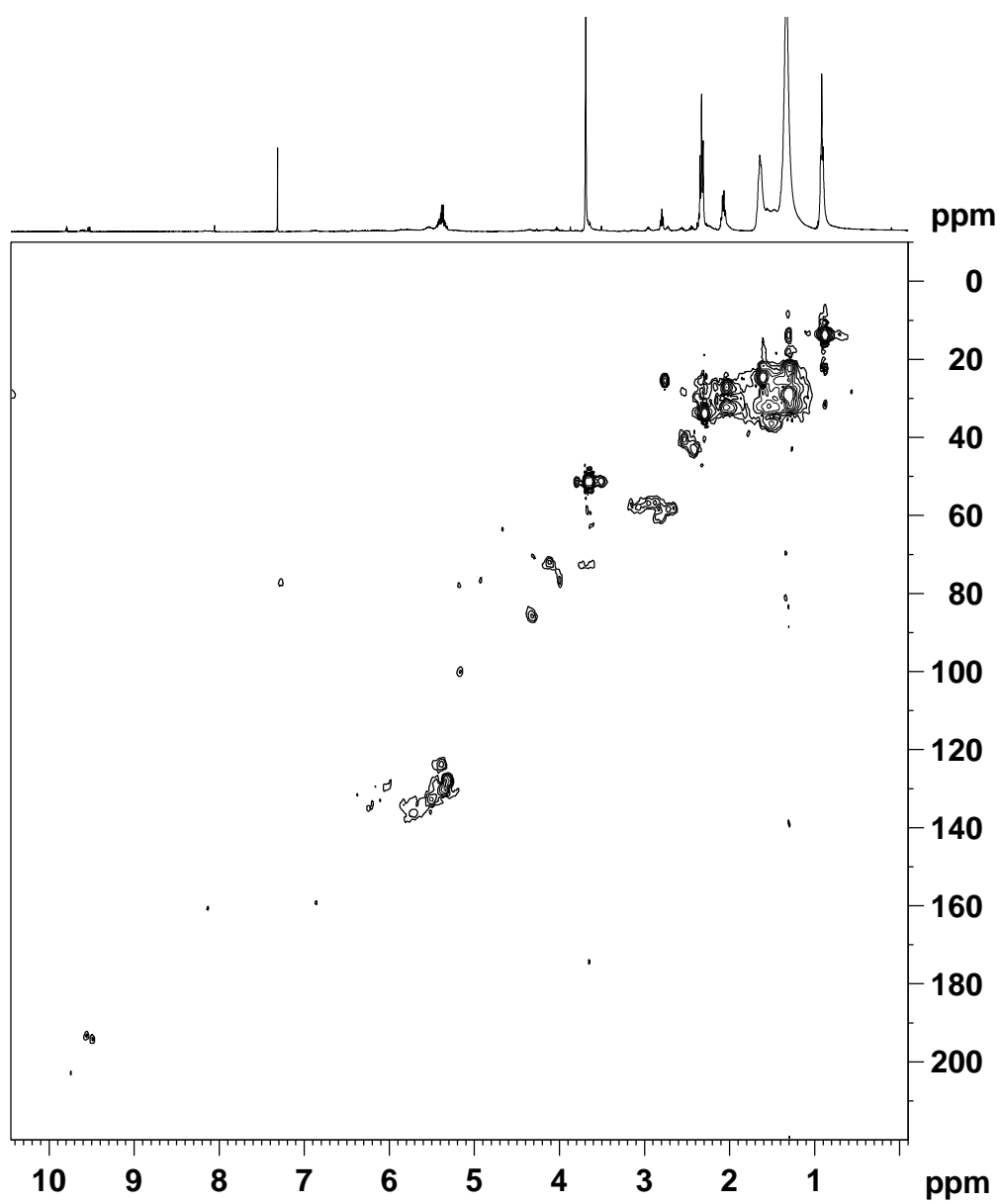
4 Fig. S1 COSY PLOT of 18:2 after 500 minutes reaction time



5

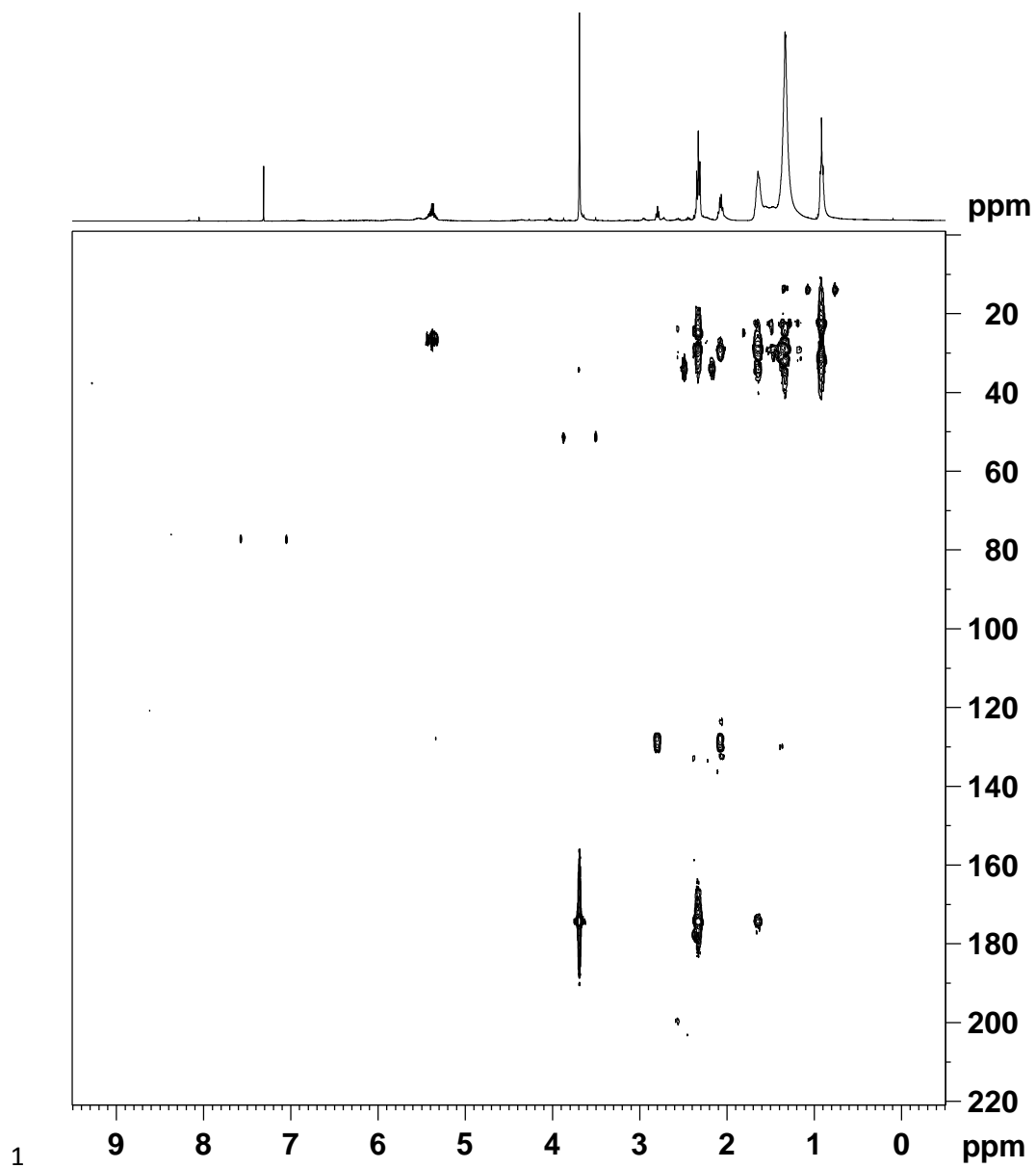
1 Fig. S2 D<sub>2</sub>O shake demonstrating that none of this region corresponds to a hydroxyl proton.

2



3

4 Fig. S3 HSQC PLOT of 18:2 after 500 minutes reaction time



1  
2 Fig. S4 HMBC PLOT of 18:2 after 500 minutes reaction time

3

4